This paper is published as part of a *Dalton Transactions* themed issue on:

Bioorganometallic Chemistry

Guest Editor Charles Riordan
University of Delaware, USA

Published in issue 22, 2009 of *Dalton Transactions*

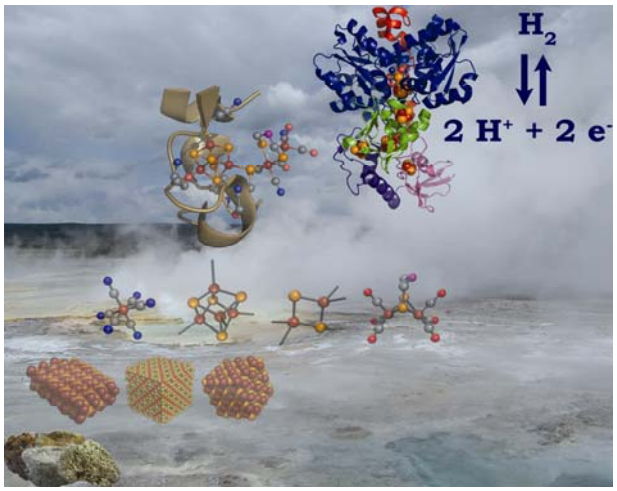

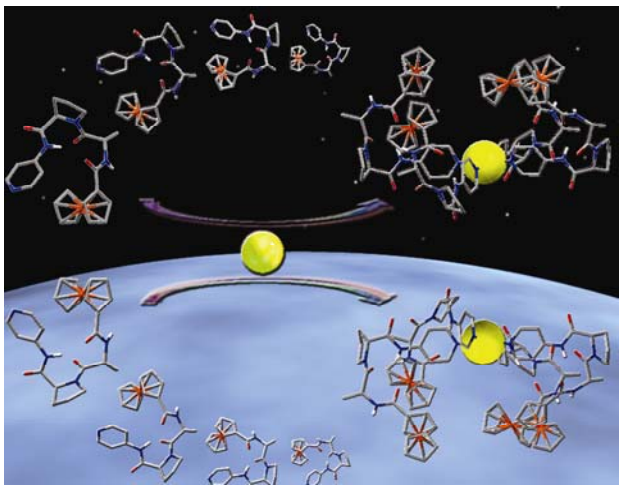

Images reproduced with permission of John Peters (left) and Toshikazu Hirao (right)

Papers published in this issue include:

Perspective: Hydrogenase cluster biosynthesis: organometallic chemistry nature's way
Shawn E. McGlynn, David W. Mulder, Eric M. Shepard, Joan B. Broderick and John W. Peters
Dalton Trans., 2009, 4274, DOI: 10.1039/b821432h

Role of aromatic substituents on the antiproliferative effects of diphenyl ferrocenyl butene compounds
Ouardia Zekri, Elizabeth A. Hillard, Siden Top, Anne Vessières, Pascal Pigeon, Marie-Aude Plamont, Michel Huché, Sultana Boutamine, Michael J. McGlinchey, Helge Müller-Bunz and Gérard Jaouen, *Dalton Trans*., 2009, 4318, DOI: 10.1039/b819812h

Resin-bound models of the [FeFe]-hydrogenase enzyme active site and studies of their reactivity
Kayla N. Green, Jennifer L. Hess, Christine M. Thomas and Marcetta Y. Darensbourg
Dalton Trans., 2009, 4344, DOI: 10.1039/b823152d

Molecular structures of protonated and mercurated derivatives of thimerosal
Wesley Sattler, Kevin Yurkerwich and Gerard Parkin
Dalton Trans., 2009, 4327, DOI: 10.1039/b823467a

Critical aspects of [NiFe]hydrogenase ligand composition
Koji Ichikawa, Takahiro Matsumoto and Seiji Ogo
Dalton Trans., 2009, 4304, DOI: 10.1039/b819395a

Visit the *Dalton Transactions* website for more cutting-edge inorganic and organometallic research
www.rsc.org/dalton

and for more bioinorganic and biological inorganic chemistry papers in *Dalton Transactions*:
www.rsc.org/Publishing/Journals/dt/News/BIB.asp

Molecular structures of protonated and mercurated derivatives of thimerosal†

Wesley Sattler, Kevin Yurkerwich and Gerard Parkin*

Received 5th January 2009, Accepted 11th February 2009
First published as an Advance Article on the web 11th March 2009
DOI: 10.1039/b823467a

The carboxylate oxygen of thimerosal, [(Ar^{CO_2})SHgEt]Na, is subject to facile electrophilic attack by H^+ and $[HgEt]^+$ to give (Ar^{CO_2H})SHgEt and [(Ar^{CO_2HgEt})SHgEt]$_2$, respectively. X-Ray diffraction demonstrates that (Ar^{CO_2H})SHgEt exists as a hydrogen bonded dimer in the solid state whereas [(Ar^{CO_2HgEt})SHgEt]$_2$ is tetranuclear, with the mercury centers being connected by bridging carboxylate groups. ^{1}H NMR spectroscopic studies indicate that the form of the ^{199}Hg satellites of the ethyl group of (Ar^{CO_2H})SHgEt are dependent on the magnetic field, such that the inner pair of CH_2 and CH_3 satellites appear as a singlet at 400 MHz, as a consequence of $^2J_{Hg-H}$ and $^3J_{Hg-H}$ having opposite signs and the difference in chemical shifts of the central CH_2 and CH_3 groups being equal to $\frac{1}{2}\{|^2J_{Hg-H} - {}^3J_{Hg-H}|\}$.

Introduction

Thimerosal, *i.e.* sodium ethylmercury thiosalicylate, [(Ar^{CO_2})SHgEt]Na, (Fig. 1),[1] is a pharmaceutical ingredient that was introduced in the 1930s under the trade name Merthiolate,[2] and subsequently found applications in a variety of products such as: vaccine preservatives; antiseptics; contact lens cleaners; soap-free cleansers; cosmetics; eye, nose and ear drops; and skin test antigens.[1,3] Furthermore, thimerosal is also widely used in biomedical studies as a sulfhydryl reagent, a calcium mobilizing agent and a cell function-modulating agent.[4] In view of the many applications, and the controversy surrounding its use as a vaccine preservative,[5–9] it is rather surprising that there are very few reports pertaining to the chemistry of thimerosal.[10] Indeed, we only recently determined the molecular structure of thimerosal by X-ray diffraction.[11] Here, we report the structural characterization of the protonated and mercurated derivatives (Ar^{CO_2H})SHgEt and [(Ar^{CO_2HgEt})SHgEt]$_2$.

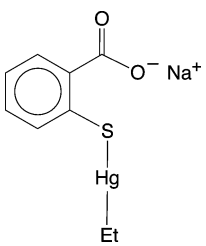

Fig. 1 Thimerosal.

Results and discussion

Protonation of thimerosal

Thimerosal possesses several sites that may be subject to electrophilic attack, two of which include the carboxylate oxygen and the mercury–carbon bond. It is, therefore, noteworthy that treatment of an aqueous solution of thimerosal with HCl(aq) results in selective protonation at the carboxylate oxygen to precipitate the carboxylic acid derivative (Ar^{CO_2H})SHgEt (Scheme 1),[12] with the mercury–carbon bond remaining intact. Since thimerosal is considered to enter cells *via* its protonated form,[4] it is particularly pertinent to compare the molecular structure of thimerosal with that of (Ar^{CO_2H})SHgEt. In this regard, X-ray diffraction studies

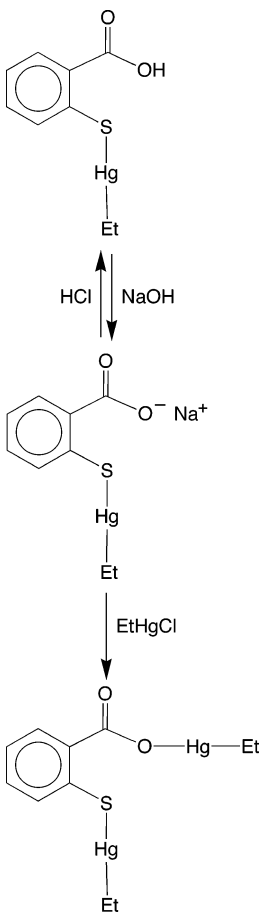

Scheme 1

Department of Chemistry, Columbia University, New York, New York 10027, USA. E-mail: parkin@columbia.edu

† CCDC reference numbers 715330–715332. For crystallographic data in CIF or other electronic format see DOI: 10.1039/b823467a

Table 1 Comparison of the mercury coordination geometries in $(Ar^{CO_2H})SHgEt$ and $[(Ar^{CO_2})SHgEt]Na$

	$(Ar^{CO_2H})SHgEt$ modification #1	$(Ar^{CO_2H})SHgEt$[a] modification #2	$[(Ar^{CO_2})SHgEt]Na$[b]
Hg–C/Å	2.086(5)	2.093[4]	2.092[21]
Hg–S/Å	2.380(1)	2.383[5]	2.375[11]
C–Hg–S/°	175.4(1)	173[2]	176[2]

[a] Average values for 4 crystallographically independent molecules; numbers in brackets represent the standard deviation. [b] Average values for 6 crystallographically independent molecules (see ref. 11); numbers in brackets represent the standard deviation.

on two crystalline forms of $(Ar^{CO_2H})SHgEt$ indicate that the compound exists as a centrosymmetric dimer involving hydrogen bonding interactions between the carboxylic acid groups, as illustrated in Figs. 2 and 3. This dimeric structure provides an interesting contrast to the complex network observed for thimerosal, which consists of $[(Ar^{CO_2})SHgEt]^-$ anions connected to Na^+ cations *via* both the oxygen and sulfur atoms of the thiosalicylate ligand.[11] The geometrical features at mercury in both crystalline forms of $(Ar^{CO_2H})SHgEt$ are, nevertheless, similar to those of thimerosal, as summarized by the data in Table 1.

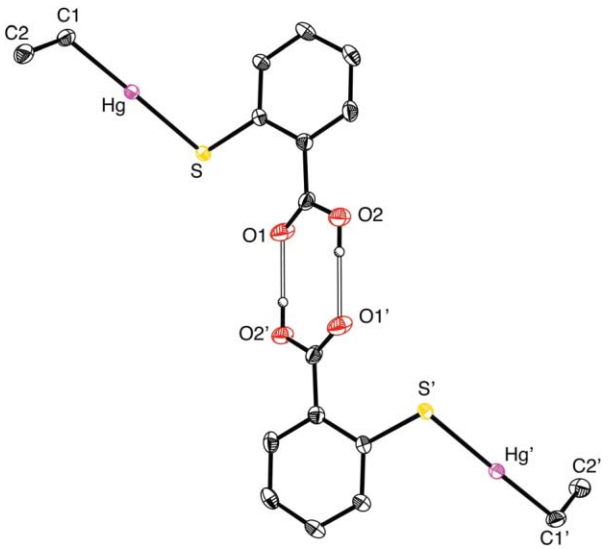

Fig. 2 Molecular structure of $(Ar^{CO_2H})SHgEt$ for modification #1 (30% thermal parameters; hydrogen atoms on carbon are omitted for clarity).

$(Ar^{CO_2H})SHgEt$ has also been characterized in solution by ^1H NMR spectroscopy, which provides evidence for both the mercury ethyl moiety and the carboxylic proton. With respect to the ethyl group, the ^1H NMR chemical shift for the CH_2 group is downfield of the CH_3 group (Fig. 4), a sequence that is in accord with that for thimerosal and other EtHgX derivatives (*e.g.* X = Cl, Br, I, ClO_4), but opposite to that of Et_2Hg.[13,14]

A particularly interesting feature of the ^1H NMR spectrum of $(Ar^{CO_2H})SHgEt$ is associated with the ^{199}Hg satellites of the ethyl group (Fig. 4). Specifically, while the outermost satellites for the CH_2 and CH_3 groups have a similar appearance to their respective central signals, the innermost satellites appear as a sharp *singlet* at 400 MHz. The origin of the singlet is that the satellites correspond to the A_2B_3 portion of an A_2B_3X spin system and, as such, their

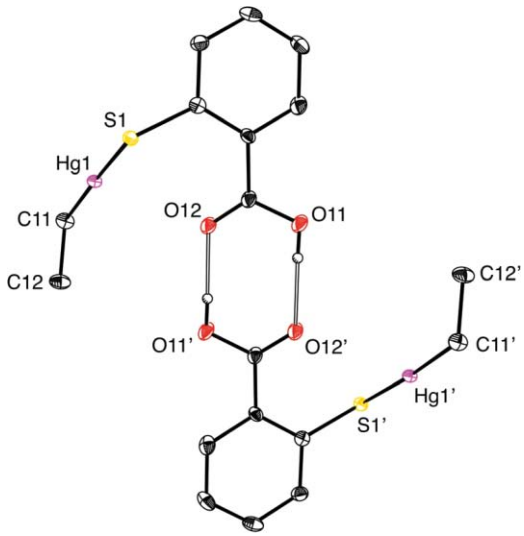

Fig. 3 Molecular structure of one of the independent molecules of $(Ar^{CO_2H})SHgEt$ for modification #2 (40% thermal parameters; hydrogen atoms on carbon are omitted for clarity).

appearance depends critically on the $J_{A\text{-}X}$ (*i.e.* $^2J_{Hg\text{-}H}$) and $J_{B\text{-}X}$ (*i.e.* $^3J_{Hg\text{-}H}$) coupling constants. If $\Delta\delta$ is the chemical shift difference ($|\delta_A - \delta_B|$) of the CH_2 and CH_3 groups for molecules devoid of magnetically active ^{199}Hg nuclei, the "effective" chemical shift difference $\Delta\delta'$ for those with the two spin states of ^{199}Hg is $|\Delta\delta \pm \frac{1}{2}(J_{A\text{-}X} - J_{B\text{-}X})|$,[15,16] as illustrated in Fig. 5. Thus, the satellites will only have a first-order appearance if $|\Delta\delta \pm \frac{1}{2}(J_{A\text{-}X} - J_{B\text{-}X})| >> |J_{AB}|$, and complex spectra for the satellites will result if this inequality is not maintained.[15,16]

In the extreme that $|\Delta\delta \pm \frac{1}{2}(J_{A\text{-}X} - J_{B\text{-}X})|$ is zero, *i.e.* $\Delta\delta = \frac{1}{2}|J_{A\text{-}X} - J_{B\text{-}X}|$, the corresponding A_2B_3 subspectra will become a singlet. While ethyl groups are not commonly observed as singlets in ^1H NMR spectra, such situations do arise if the CH_2 and CH_3 groups coincidentally have the same chemical shift; for example, the silicon ethyl groups of $[Tp^{Me_2}]Pt(H)_2Si(CH_2CH_3)_3$ appear as a singlet in the ^1H NMR spectrum.[17,18] Most interestingly, the ^{29}Si satellites, however, appear as triplet and quartet signals because the different $^2J_{Si\text{-}H}$ and $^3J_{Si\text{-}H}$ coupling constants effectively remove the coincidental chemical shift degeneracy.[19] A similar effect has also been observed in the $^{31}P\{^1H\}$ NMR spectrum of Pt[(*R*,*R*)-Me-Duphos][$CH_2CH(CO_2Bu^t)$], for which the central signal is observed as a singlet due to the coincidental equivalence of the chemical shifts of the two different phosphorus nuclei, but coupling is observed in the ^{195}Pt satellite signals due to the $J_{Pt\text{-}P}$ coupling constants having different values.[20,21]

The observation that it is the "inner" pair of satellites which exhibits the second-order behaviour indicates that $J_{A\text{-}X}$ (*i.e.* $^2J_{Hg\text{-}H}$) and $J_{B\text{-}X}$ (*i.e.* $^3J_{Hg\text{-}H}$) have opposite signs.[15,16,22] In this regard, if $J_{A\text{-}X}$ and $J_{B\text{-}X}$ were to have the same sign, an "outer" pair of satellites would exhibit the second-order behaviour if the requirement $\Delta\delta = \frac{1}{2}|J_{A\text{-}X} - J_{B\text{-}X}|$ were to be satisfied. For example, an outer pair of ^{195}Pt satellites appear as a singlet in the $^{31}P\{^1H\}$ NMR spectrum of $[\{Pt(OP(OMe)_2]_2dppe\}_2Zn]^{2+}$ because the two $J_{Pt\text{-}P}$ coupling constants have the same sign.[23] The notion that $^2J_{Hg\text{-}H}$ and $^3J_{Hg\text{-}H}$ for $(Ar^{CO_2H})SHgEt$ have different signs is in accord with other studies, which suggest that the former is negative, while the latter is positive.[22]

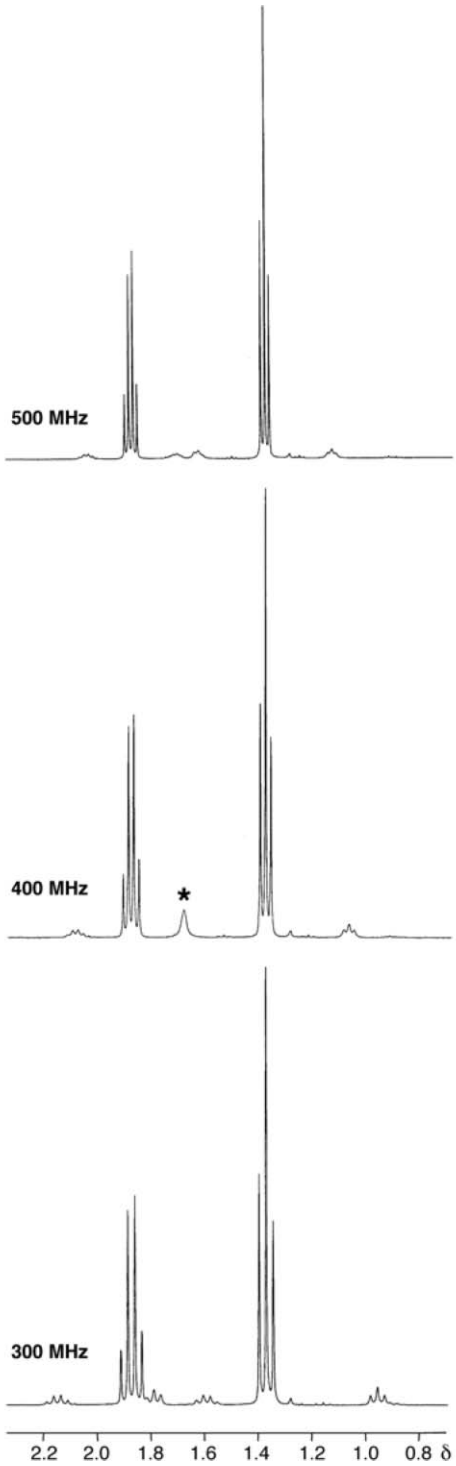

Fig. 4 ^{1}H NMR spectra of (Ar^{CO_2H})SHgEt as a function of magnetic field. At 400 MHz, the central pair of ^{199}Hg satellites appear as a singlet (*).

As a consequence of the fact that the chemical shift difference (when expressed in terms of Hz) of the CH_2 and CH_3 groups is a function of the magnetic field, the "effective" chemical shift differences $\Delta\delta'$ for the A_2B_3 satellites subspectra are also field dependent. Thus, while the signals of the CH_2 and CH_3 satellites of (Ar^{CO_2H})SHgEt fortuitously overlap at 400 MHz to give a singlet, more complex spectra are observed at both 300 MHz and 500 MHz

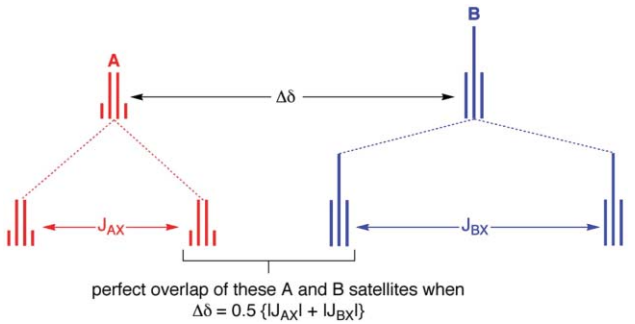

Fig. 5 Schematic illustration of the ^{199}Hg satellites for a mercury ethyl group. The two inner satellites overlap if $\Delta\delta = \frac{1}{2}\{|J_{A\text{-}X}| + |J_{B\text{-}X}|\}$. If $J_{A\text{-}X}$ and $J_{B\text{-}X}$ have opposite signs, the two satellites correspond to the same molecule and so a singlet results.

(Fig. 4). EtHgCl also exhibits similar field-dependent satellites, with a singlet being observed for the inner satellites at 400 MHz (Fig. 6). The derived coupling constant data for (Ar^{CO_2H})SHgEt and EtHgCl[24] are summarized in Table 2, which also includes the data for thimerosal. In each case, the absolute magnitude of $|^{2}J_{Hg\text{-}H}|$ is smaller than $|^{3}J_{Hg\text{-}H}|$, a trend that is also observed for other EtHgX derivatives.[25]

One final noteworthy aspect concerned with the mercury satellites of (Ar^{CO_2H})SHgEt is that the coupling is not as well resolved as that for the central signals. The origin of this effect is relaxation by chemical shift anisotropy (CSA),[26] an effect that is of considerable importance for compounds with ^{199}Hg in a linear environment, for which the chemical shift anisotropy is large.[27] In this regard, we previously attributed the pronounced line broadening of the mercury satellites of thimerosal to CSA.[11]

Stability of (Ar^{CO_2H})SHgEt with respect to protolytic cleavage of the Hg–C bond

While it is evident that protonation of the carboxylate oxygen atom of thimerosal is kinetically more facile than protonation of the Hg–C bond, the latter would ultimately be expected to give the more thermodynamically favoured products.[28] Indeed, since protonation of the carboxylate oxygen is reversible (Scheme 1), it indicates that there is a significant barrier towards protolytically cleaving the Hg–C bond of thimerosal. Likewise, it is also thermodynamically possible that the Hg–C bond of (Ar^{CO_2H})SHgEt could be cleaved in an intermolecular manner by the carboxylic acid group of another molecule of (Ar^{CO_2H})SHgEt, but (Ar^{CO_2H})SHgEt is resistant to such cleavage. For example, (Ar^{CO_2H})SHgEt is stable with respect to elimination of ethane at 150 °C over a period of 3 d. The kinetic stability of (Ar^{CO_2H})SHgEt is, nevertheless, in accord with the notion that two-coordinate mercury alkyl compounds are generally not susceptible to protolytic cleavage.[29] However, while these observations indicate that the Hg–C bonds of both thimerosal and its protonated derivative are not *per se* subject to facile protolytic cleavage, it must be recognized that suitable donor ligands and different Brønsted acids could promote the cleavage. In this regard, we have recently demonstrated that addition of 1-*t*-butyl-2-mercaptoimidazole, $Hmim^{Bu^t}$, to a mixture of {[$Hmim^{Bu^t}$]HgEt}[BF_4] and PhSH causes elimination of ethane at room temperature.[29]

Table 2 ^{1}H NMR chemical shift and coupling constant data for mercury ethyl complexes.[a]

	Solvent	$\delta(CH_2)$/ppm	$\delta(CH_3)$/ppm	$^{2}J_{Hg-H}$/Hz	$^{3}J_{Hg-H}$/Hz
$(Ar^{CO_2H})SHgEt$	$CDCl_3$	1.89 $^{3}J_{H-H} = 8$ Hz	1.35 $^{3}J_{H-H} = 8$ Hz	−168	+252
$[(Ar^{CO_2HgEt})SHgEt]_2$	CD_2Cl_2	1.83 $^{3}J_{H-H} = 8$ Hz	1.32 $^{3}J_{H-H} = 8$ Hz	−193	+273
$[(Ar^{CO_2})SHgEt]Na$[b]	D_2O	1.65 $^{3}J_{H-H} = 8$ Hz	1.26 $^{3}J_{H-H} = 8$ Hz	|176|	|250|
EtHgCl	CD_2Cl_2	1.98 $^{3}J_{H-H} = 8$ Hz	1.35 $^{3}J_{H-H} = 8$ Hz	−202	+292

[a] Where indicated, the relative signs are determined by analysis of the data, but the absolute sign is based on comparison with the literature (ref. 22). [b] Data taken from ref. 11.

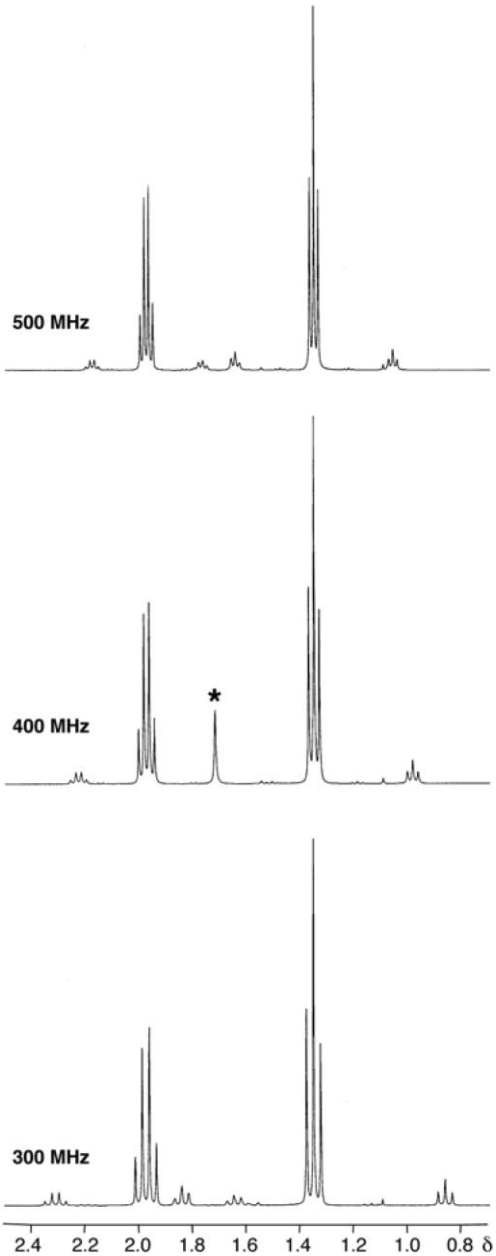

Fig. 6 ^{1}H NMR spectra of EtHgCl as a function of magnetic field. At 400 MHz, the central pair of ^{199}Hg satellites appear as a singlet (*).

Mercuration of thimerosal

In addition to protonation, the carboxylate oxygen may be mercurated by addition of EtHgCl to give $[(Ar^{CO_2HgEt})SHgEt]_2$ (Scheme 1).[30] The synthesis of this complex is significant because a compound with the corresponding empirical formula has been reported to be an unexpected impurity in the synthesis of thimerosal.[10a] While there is a close formal analogy between addition of H^+ and $[EtHg]^+$ to $[(Ar^{CO_2})SHgEt]^-$, the structure of the products differ considerably. Specifically, X-ray diffraction demonstrates that addition of $[EtHg]^+$ to thimerosal results in a species with a complex tetranuclear structure, $[(Ar^{CO_2HgEt})SHgEt]_2$, that features both three- and four-coordinate mercury centers. The mercury centers are linked by carboxylate groups, with each one serving to bridge three mercury centers, as illustrated in Fig. 7. The Hg–O distances, however, span the substantial range 2.13–2.80 Å (Table 3), with the principal Hg–O interaction being *trans* to the ethyl group. As such, the mercury coordination environments are best described as being two-coordinate linear centers supplemented by secondary interactions.[31] Interestingly, despite the fact that $[(Ar^{CO_2HgEt})SHgEt]_2$ possesses two chemically distinct [HgEt] moieties, ^{1}H NMR spectroscopy (Table 2) indicates

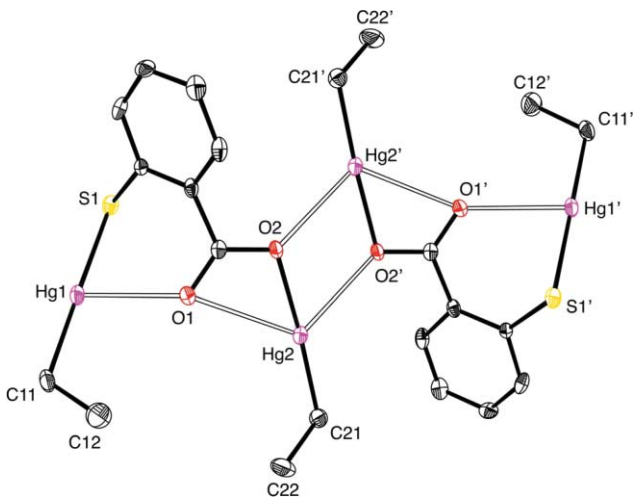

Fig. 7 Molecular structure of $[(Ar^{CO_2HgEt})SHgEt]_2$ (30% thermal parameters; hydrogen atoms on carbon are omitted for clarity).

Table 3 Selected bond lengths for $[(Ar^{CO_2HgEt})SHgEt]_2$

	d(Hg–X)/Å
Hg1–C11	2.099(10)
Hg2–C21	2.074(9)
Hg1–S1	2.382(2)
Hg1–O1	2.596(6)
Hg2–O2′	2.751(6)
Hg2–O1	2.799(6)
Hg2–O2	2.132(6)

the presence of only *one* chemically distinct mercury ethyl group. Assuming that the equivalence is not coincidental, a plausible explanation to account for the observation of a single mercury ethyl group is chemical exchange involving dissociation of $[HgEt]^+$.

Conclusions

In summary, thimerosal is protonated selectively by HCl at the carboxylate oxygen atom to give the mercury ethyl derivative $(Ar^{CO_2H})SHgEt$, rather than cleave the Hg–Et bond and eliminate ethane. The carboxylate oxygen is also subject to electrophilic attack by $[HgEt]^+$ to give $[(Ar^{CO_2HgEt})SHgEt]_2$. Despite the formal similarity of the reactions involving H^+ and $[HgEt]^+$, however, the protonated derivative $(Ar^{CO_2H})SHgEt$ exists as a hydrogen bonded dimer in the solid state, while $[(Ar^{CO_2HgEt})SHgEt]_2$ is tetranuclear, with the mercury centers being connected by bridging carboxylate groups.

Experimental

General considerations

All manipulations were performed using a combination of glovebox, high-vacuum and Schlenk techniques under a nitrogen or argon atmosphere, except where otherwise stated. Solvents were purified and degassed by standard procedures. NMR spectra were measured on Bruker 300 DRX, Bruker 400 DRX and Bruker Avance 500 DMX spectrometers. ^{1}H NMR spectra are reported in ppm relative to $SiMe_4$ ($\delta = 0$) and were referenced internally with respect to the protio solvent impurity (δ 7.26 for $CDCl_3$[32] and 5.32 for CD_2Cl_2[33]). ^{13}C NMR spectra are reported in ppm relative to $SiMe_4$ ($\delta = 0$) and were referenced internally with respect to the solvent ($\delta = 39.52$ for DMSO).[32] ^{199}Hg NMR chemical shifts are reported relative to $HgMe_2$ ($\delta = 0$) but in view of the toxicity of the latter compound, the spectra were referenced externally with respect to HgI_2 (1 M in d^6-DMSO, $\delta = -3106$).[34] Coupling constants are given in hertz. IR spectra were recorded as KBr pellets on a Nicolet Avatar DTGS spectrometer, and the data are reported in reciprocal centimeters. Thimerosal (Acros) and EtHgCl (Strem) were obtained commercially.

Synthesis of $(Ar^{CO_2H})SHgEt$

A solution of thimerosal (200 mg, 0.49 mmol) in water (5 mL) was treated with HCl_{aq} (0.040 mL of 12.2 M, 0.49 mmol), resulting in the immediate formation of a white precipitate, which was extracted into CH_2Cl_2 (7 mL). The dichloromethane extract was washed with water (3 × 3 mL) and the volatile components were then removed *in vacuo* to give $(Ar^{CO_2H})SHgEt$ as a white solid (147 mg, 79%). Anal. calcd for $(Ar^{CO_2H})SHgEt$: C 28.2%, H 2.6%. Found: C 28.3%, H 2.6%. ^{1}H NMR ($CDCl_3$): 1.35 [t, $^3J_{H-H} = 8$, $^3J_{H-Hg} = 252$, 3 H of $HO_2CC_6H_4SHgCH_2CH_3$], 1.89 [q, $^3J_{H-H} = 8$, $^2J_{H-Hg} = 168$, 2 H of $HO_2CC_6H_4SHgCH_2CH_3$], 7.30 [t, $^3J_{H-H} = 8$, 1 H of $HO_2CC_6H_4SHgCH_2CH_3$], 7.39 [t, $^3J_{H-H} = 8$, 1 H of $HO_2CC_6H_4SHgCH_2CH_3$], 7.61 [d, $^3J_{H-H} = 8$, 1 H of $HO_2CC_6H_4SHgCH_2CH_3$], 8.25 [d, $^3J_{H-H} = 8$, 1 H of $HO_2CC_6H_4SHgCH_2CH_3$], 11.79 [s, 1 H of $HO_2CC_6H_4SHgCH_2CH_3$]. ^{13}C NMR (DMSO): 13.7 [q, $^1J_{C-H} = 124$, $^2J_{Hg-C} = 73$, 1 C of $HO_2CC_6H_4SHgCH_2CH_3$], 25.4 [t, $^1J_{C-H} = 132$, $^1J_{Hg-C} = 1362$, 1 C of $HO_2CC_6H_4SHgCH_2CH_3$], 124.4 [d, $^1J_{C-H} = 163$, 1 C of $HO_2CC_6H_4SHgCH_2CH_3$], 128.6 [d, $^1J_{C-H} = 161$, 1 C of $HO_2CC_6H_4SHgCH_2CH_3$], 129.9 [d, $^1J_{C-H} = 160$, 1 C of $HO_2CC_6H_4SHgCH_2CH_3$], 135.4 [d, $^1J_{C-H} = 161$, 1 C of $HO_2CC_6H_4SHgCH_2CH_3$], 136.2 [s, 1 C of $HO_2CC_6H_4SHgCH_2CH_3$], 137.3 [s, 1 C of $HO_2CC_6H_4SHgCH_2CH_3$], 170.2 [s, 1 C of $HO_2CC_6H_4SHgCH_2CH_3$]. ^{199}Hg{^{1}H} NMR (DMSO): −788 [tq]. IR Data (KBr, cm^{-1}): 3066 (s), 2963 (s), 2942 (s), 2909 (s), 2856 (s), 2725 (m), 2638 (m), 2544 (m), 1921 (w), 1692 (vs), 1589 (m), 1556 (m), 1468 (s), 1424 (m), 1403 (vs), 1302 (s), 1282 (s), 1251 (vs), 1172 (m), 1138 (m), 1109 (w), 1049 (s), 1032 (m), 946 (w), 902 (m), 809 (m), 787 (w), 732 (vs), 708 (m), 696 (m), 643 (m).

Deprotonation of $(Ar^{CO_2H})SHgEt$

A suspension of $(Ar^{CO_2H})SHgEt$ (20 mg, 0.052 mmol) in D_2O was treated with NaOH (0.28 mL of 0.225 M NaOH in D_2O, 0.063 mmol), thereby resulting in the formation of a solution. The sample was monitored by ^{1}H NMR spectroscopy which demonstrated the formation of $[(Ar^{CO_2})SHgEt]Na$.

Thermal stability of $(Ar^{CO_2H})SHgEt$

(a) A solution of $(Ar^{CO_2H})SHgEt$ (*ca.* 20 mg) in $CDCl_3$ (*ca.* 0.7 mL) was heated at 150 °C. The sample was monitored by ^{1}H NMR spectroscopy which demonstrated that $(Ar^{CO_2H})SHgEt$ is stable with respect to elimination of ethane over a period of 3 d.

(b) A solution of $(Ar^{CO_2H})SHgEt$ (*ca.* 20 mg) in CD_3OD (*ca.* 0.7 mL) was heated at 140 °C. The sample was monitored by ^{1}H NMR spectroscopy which demonstrated that $(Ar^{CO_2H})SHgEt$ is stable with respect to elimination of ethane over a period of 12 h.

Synthesis of $[(Ar^{CO_2HgEt})SHgEt]_2$

A mixture of thimerosal (100 mg, 0.247 mmol) and EtHgCl (59 mg, 0.223 mmol) in water (1 mL) and methanol (2 mL) was stirred for 5 min. After this period, the mixture was filtered and the precipitate was washed sequentially with water (3 × 1 mL) and methanol (2 × 2 mL) and dried *in vacuo* to give $[(Ar^{CO_2HgEt})SHgEt]_2$ as a white solid (47 mg, 35%). Anal. calcd for $[(Ar^{CO_2HgEt})SHgEt]_2 \cdot 6H_2O$: C 19.9%, H 3.0%. Found: C 19.3%, H 2.1%. ^{1}H NMR (CD_2Cl_2): 1.32 [t, $^3J_{H-H} = 8$, $^3J_{H-Hg} = 273$, 6 H of $H_3CCH_2HgO_2CC_6H_4SHgCH_2CH_3$], 1.83 [q, $^3J_{H-H} = 8$, $^2J_{H-Hg} = 193$, 4 H of $H_3CCH_2HgO_2CC_6H_4SHgCH_2CH_3$], 7.12 [t, $^3J_{H-H} = 8$, 1 H of $H_3CCH_2HgO_2CC_6H_4SHgCH_2CH_3$, 7.21 [t, $^3J_{H-H} = 8$, 1 H of $H_3CCH_2HgO_2CC_6H_4SHgCH_2CH_3$], 7.54 [m, 2 H of $H_3CCH_2HgO_2CC_6H_4SHgCH_2CH_3$]. ^{13}C NMR (DMSO): 13.9 [q, $^1J_{C-H} = 126$, $^2J_{Hg-c} = 91$, 2 C of $H_3CCH_2HgO_2CC_6H_4SHgCH_2CH_3$], 20.7 [t, $^1J_{C-H} = 133$, $^1J_{Hg-C} = 1570$, 2 C of $H_3CCH_2HgO_2CC_6H_4SHgCH_2CH_3$], 124.4 [d, $^1J_{C-H} = 162$, 1 C of $H_3CCH_2HgO_2CC_6H_4SHgCH_2CH_3$], 127.9 [d, $^1J_{C-H} = 160$, 1 C of $H_3CCH_2HgO_2CC_6H_4SHgCH_2CH_3$], 128.6 [d, $^1J_{C-H} = 158$, 1 C of $H_3CCH_2HgO_2CC_6H_4SHgCH_2CH_3$], 135.3 [d, $^1J_{C-H} = 162$, 1 C of $H_3CCH_2HgO_2CC_6H_4SHgCH_2CH_3$], 135.5 [s, 1 C of $H_3CCH_2HgO_2CC_6H_4SHgCH_2CH_3$], 141.2 [s, 1 C of $H_3CCH_2HgO_2CC_6H_4SHgCH_2CH_3$], 173.7 [s, 1 C of $H_3CCH_2HgO_2CC_6H_4SHgCH_2CH_3$]. IR Data (KBr, cm^{-1}): 3056 (w), 3043 (w), 2973 (m), 2946 (m), 2913 (m), 2858 (m), 1600 (vs), 1577 (s), 1460 (m), 1425 (m), 1338 (vs), 1271 (m), 1254 (m), 1231 (w), 1183 (m), 1142 (m), 1115 (w), 1048 (m), 1033 (w), 960 (w), 949 (w), 857 (m), 792 (w), 752 (vs), 732 (m), 711 (m), 689 (m), 651 (m).

Table 4 Crystal, intensity collection and refinement data

	$(Ar^{CO_2H})SHgEt$ #1	$(Ar^{CO_2H})SHgEt$ #2	$[(Ar^{CO_2HgEt})SHgEt]_2$
Lattice	Monoclinic	Monoclinic	Monoclinic
Formula	$C_9H_{10}HgO_2S$	$C_9H_{10}HgO_2S$	$C_{22}H_{28}Hg_4O_4S_2$
Formula weight	382.82	382.82	1222.92
Space group	$P2_1/n$	$P2/c$	$C2/c$
a/Å	9.1662(8)	30.096(3)	22.943(3)
b/Å	5.3545(5)	4.0444(4)	7.7108(9)
c/Å	20.5095(17)	33.472(4)	15.0681(16)
α/°	90	90	90
β/°	93.666(1)	91.153(1)	94.551(2)
γ/°	90	90	90
V/Å^3	1004.6(2)	4073.4(7)	2657.2(5)
Z	4	16	8
T/K	125(2)	125(2)	125(2)
Radiation λ/Å	0.71073	0.71073	0.71073
ρ_{calcd}/g cm^{-3}	2.531	2.497	3.057
μ (MoKα)/mm^{-1}	15.492	15.282	23.222
θ max./°	32.37	31.29	32.46
No. of data	3436	13 211	4547
No. of parameters	118	469	145
R_{int}	0.0451	0.0658	0.0502
R_1 [$I > 2\sigma(I)$]	0.0291	0.0354	0.0509
wR_2 [$I > 2\sigma(I)$]	0.0835	0.0598	0.1302
GOF	1.038	1.020	1.104

X-Ray structure determinations

Single-crystal X-ray diffraction data were collected on either a Bruker Apex II diffractometer. Crystal data, data collection and refinement parameters are summarized in Table 4. The structures were solved using direct methods and standard difference map techniques, and were refined by full-matrix least-squares procedures on F^2 with SHELXTL (version 6.10).[35]

Acknowledgements

We thank the National Institutes of Health (GM046502) for support of this research. The National Science Foundation (CHE-0619638) is thanked for acquisition of an X-ray diffractometer.

References

1 D. A. Geier, L. K. Sykes and M. R. Geier, *J. Toxicol. Environ. Health*, 2007, **10**, 575–596.
2 H. M. Powell and W. A. Jamieson, *Am. J. Hygiene*, 1931, **13**, 296–310.
3 (*a*) H. Ohno, R. Doi, Y. Kashima, S. Murae, T. Kizaki, Y. Hitomi, N. Nakano and M. Harada, *Bull. Environ. Contam. Toxicol.*, 2004, **73**, 777–780; (*b*) S. Gil, I. Lavilla and C. Bendicho, *J. Anal. At. Spectrom.*, 2007, **22**, 569–572; (*c*) A. Fagundes, M. C. A. Marzochi, M. Perez, A. Schubach, A. Ferreira, J. P. Silva, T. Schubach and K. B. F. Marzochi, *Acta Tropica*, 2007, **101**, 25–30; (*d*) B. K. Meyer, A. Ni, B. Hu and L. Shi, *J. Pharm. Sci.*, 2007, **96**, 3155–3167.
4 J. G. Elferink, *Gen. Pharmacol.*, 1999, **33**, 1–6.
5 (*a*) T. W. Clarkson and L. Magos, *Crit. Rev. Toxicol.*, 2006, **36**, 609–662; (*b*) J. Mutter, J. Naumann and C. Guethlin, *Crit. Rev. Toxicol.*, 2007, **37**, 537–549; (*c*) T. W. Clarkson, *Env. Health Persp. Suppl.*, 2002, **110**, 11–23; (*d*) T. W. Clarkson, *Crit. Rev. Clin. Lab. Sci.*, 1997, **34**, 369–403; (*e*) N. J. Langford and R. E. Ferner, *J. Human Hypertension*, 1999, **13**, 651–656; (*f*) D. W. Boening, *Chemosphere*, 2000, **40**, 1335–1351; (*g*) L. Magos, *Metal Ions in Biological Systems*, 1997, **34**, 321–370; (*h*) A. R. Hutchison and D. A. Atwood, *J. Chem. Crystallogr.*, 2003, **33**, 631–645; (*i*) L. Alessio, M. Campagna and R. Lucchini, *Am. J. Ind. Med.*, 2007, **50**, 779–787; (*j*) T. W. Clarkson, J. B. Vyas and N. Ballatorl, *Am. J. Ind. Med.*, 2007, **50**, 757–764; (*k*) J. F. Risher, De and C. T. Rosa, *J. Env. Health*, 2007, **70**, 9–16; (*l*) J. C. Clifton, *Ped. Clin. North America*, 2007, **54**, 237–269.
6 (*a*) C. J. Clements and P. B. McIntyre, *Expert Opin. Drug Safety*, 2006, **5**, 17–29; (*b*) M. F. Blaxill, L. Redwood and S. Bernard, *Med. Hypoth.*, 2004, **62**, 788–794; (*c*) S. Bernard, A. Enayati, L. Redwood, H. Roger and T. Binstock, *Med. Hypoth.*, 2001, **56**, 462–471; (*d*) *Thimerosal-Containing Vaccines and Neurodevelopmental Disorders.* ed. K. Stratton, A. Gable and M. C. McCormick, National Academy Press, Washington, DC, 2001; (*e*) D. A. Geier and M. R. Geier, *J. Toxicol. Environ. Health*, 2007, **70**, 837–851.
7 (*a*) F. de Stefano, *Clin. Pharmacol. Thereapeutics*, 2007, **82**, 756–759; (*b*) P. A. Offit, *New Engl. J. Med.*, 2007, **357**, 1278–1279; (*c*) W. W. Thompson, C. Price, B. Goodson, D. K. Shay, P. Benson, V. L. Hinrichsen, E. Lewis, E. Eriksen, P. Ray, S. M. Marcy, J. Dunn, L. A. Jackson, T. A. Lieu, S. Black, G. Stewart, E. S. Weintraub, R. L. Davis and F. DeStefano, *New Engl. J. Med.*, 2007, **357**, 1281–1292.
8 (*a*) S. Bernard, *New Engl. J. Med.*, 2008, **358**, 93; (*b*) J. P. K. Rooney, *New Engl. J. Med.*, 2008, **358**, 93–94; (*c*) W. W. Thompson, C. Price and F. DeStafano, *New Engl. J. Med.*, 2008, **358**, 94.
9 J. P. Baker, *Am. J. Public Health*, 2008, **98**, 2–11.
10 (*a*) V. M. Trikojus, *Nature*, 1946, **158**, 472–473; (*b*) M. Tan and J. E. Parkin, *Int. J. Pharm.*, 2000, **208**, 23–34; (*c*) X. Wu, H. Liang, K. A. O'Hara, J. C. Yalowich and B. B. Gasinoff, *Chem. Res. Toxicol.*, 2008, **21**, 483–493.
11 J. G. Melnick, K. Yurkerwich, D. Buccella, W. Sattler and G. Parkin, *Inorg. Chem.*, 2008, **47**, 6421–6426.
12 (*a*) $(Ar^{CO_2H})SHgEt$ has been previously described without any detailed characterization. See: J. H. Waldo, *J. Am. Chem. Soc.*, 1931, **53**, 992–996; (*b*) M. S. Kharasch, Alkyl Merucric Sulfur Compound and Process for Producing It, *US Pat. #1*, 1928, **672**, 615.
13 D. F. Evans and J. P. Maher, *J. Chem. Soc.*, 1962, 5125–5128.
14 (*a*) It is worth noting that the opposite trend for the chemical shifts of the CH_2 and CH_3 groups of Et_2Hg has also been reported and this presumably reflects the adoption of a chemical shift scale that is different to the δ scale. See: V. S. Petrosya and O. A. Reutov, *J. Organomet. Chem.*, 1974, **76**, 123–169; (*b*) J. V. Hatton, W. G. Schneider and W. Siebrand, *J. Chem. Phys.*, 1963, **39**, 1330–1336.
15 P. T. Narasimhan and M. T. Rogers, *J. Chem. Phys.*, 1959, **31**, 1430.
16 (*a*) For other examples of second-order satellite subspectra for $[XCH_2CH_3]$ compounds, see: P. T. Narasimhan and M. T. Rogers, *J. Chem. Phys.*, 1951, **34**, 1049–1055; (*b*) S. F. A. Kettle, *J. Chem. Soc.*, 1965, 6664–6665; (*c*) G. Hamer and A. Shaver, *Can. J. Chem.*, 1980, **58**, 2011–2015; (*d*) P. A. Scherr and J. P. Oliver, *J. Am. Chem. Soc.*, 1972, **94**, 8026–8031.

17 S. Reinartz, P. S. White, M. Brookhart and J. L. Templeton, *Organometallics*, 2000, **19**, 3748–3750.
18 For a vinyl compound in which the three hydrogen atoms appear as a singlet, see: I. M. Al-Najaar and M. Green, *Trans. Met. Chem.*, 1978, **3**, 142–144.
19 M. Brookhart, personal communication.
20 D. S. Glueck, *Coord. Chem. Rev.*, 2008, **252**, 2171–2179.
21 For a related examples, see: E. W. Kalberer and D. M. Roddick, *Organometallics*, 2004, **23**, 4209–4214.
22 F. A. L. Anet and J. L. Sudmeier, *J. Magn. Reson.*, 1969, **1**, 124–138.
23 R. P. Sperline, W. B. Beaulieu and D. M. Roundhill, *Inorg. Chem.*, 1978, **17**, 2032–2035.
24 The coupling constants for EtHgCl are comparable to the values of $^{2}J_{H-H} = -222$ Hz and $^{3}J_{H-H} = +300$ Hz measured using a 60 MHz spectrometer.
25 V. S. Petrosya and O. A. Reutov, *J. Organomet. Chem.*, 1974, **76**, 123–169.
26 (*a*) T. C. Farrar, E. D. Becker, *Pulse and FT NMR*, Academic Press, New York, 1971; (*b*) T. C. Farrar, *Introduction to Pulse NMR Spectroscopy*, The Farragut Press, Chicago, Madison, 1989; (*c*) R. Thouvenot, *L'Actualite Chimique*, 1996, 7, 102-111; (*d*) J. Kowalewski, L. Mäler, *Nuclear Spin Relaxation in Liquids: Theory, Experiments, and Applications*, Taylor and Francis, New York, 2006.
27 (*a*) For other examples of relaxation by chemical shift anisotropy in mercury compounds, see: R. Benn, H. Günther, A. Maercker, V. Menger and P. Schmitt, *Angew. Chem., Int. Ed. Engl.*, 1982, **21**, 295–296; (*b*) D. G. Gillies, L. P. Blaauw, G. R. Hays, R. Huis and A. D. H. Clague, *J. Magn. Reson.*, 1981, **42**, 420–428; (*c*) F. Cecconi, C. A. Ghilardi, P. Innocenti, S. Midollini, A. Orlandini, A. Ienco and A. Vacca, *J. Chem. Soc., Dalton Trans.*, 1996, 2821–2826; (*d*) R. E. Wasylishen, R. E. Lenkinski and C. Rodger, *Can. J. Chem.*, 1982, **60**, 2113–2117.
28 See, for example: T. R. Cundari and A. Yoshikawa, *J. Comput. Chem.*, 1998, **19**, 902–911.
29 J. G. Melnick and G. Parkin, *Science*, 2007, **317**, 225–227, and references therein.
30 A zinc derivative of thimerosal has been described, although no spectroscopic or structural data were reported. See: J. Birner and J. R. Garnet, *J. Pharm. Sci.*, 1964, **53**, 1266–1267.
31 (*a*) J. S. Casa, M. S. García-Tasende and J. Sordo, *Coord. Chem. Rev.*, 1999, **193–195**, 283–359; (*b*) C. E. Holloway and M. Melník, *J. Organomet. Chem.*, 1995, **495**, 1–31.
32 H. E. Gottlieb, V. Kotlyar and A. Nudelman, *J. Org. Chem.*, 1997, **62**, 7512–7515.
33 Cambridge Isotope Laboratories, Inc., NMR Solvent Data Chart (http://www.isotope.com/cil/products/images/nmrchart.pdf).
34 R. G. Kidd, R. J. Goodfellow, in *NMR and The Periodic Table*, ed. R. K. Harris, B. E. Mann, Academic Press, New York, 1978, p. 268.
35 (*a*) G. M. Sheldrick, *Acta Crystallogr., Sect. A: Found. Crystallogr.*, 2008, **64**, 112–122.